yellow. The cadmium nitrite salts can be said to be colorless, in contrast with the bright-yellow color of $Pb(NO_2)_2.H_2O$ and $Hg_2(NO_2)_2$ crystals. The present study confirmed that the perturbation of the NO_2^- by the Cd^{2+} ion is too small to give coloration.

References

HAMILTON, W. C. (1959). *Acta Cryst.* **12**, 609–610.

International Tables for X-ray Crystallography (1974). Vol. IV, pp. 72–98, 102, 149–150. Birmingham: Kynoch Press. (Present distributor Kluwer Academic Publishers, Dordrecht.)

MCGLYNN, S. P., AZUMI, T. & KUMAR, D. (1981). *Chem. Rev.* **81**, 475–489.

OHBA, S., KIKKAWA, T. & SAITO, Y. (1985). *Acta Cryst.* C**41**, 10–13.

OHBA, S., MATSUMOTO, F., TAKAZAWA, H. & SAITO, Y. (1987). *Acta Cryst.* C**43**, 191–194.

SAKURAI, T. & KOBAYASHI, K. (1979). *Rikagaku Kenkyusho Hokoku*, **55**, 69–77.

Acta Cryst. (1988). C**44**, 1707–1709

Electron Difference Density in Potassium Zinc Fluoride Perovskite

BY R. H. BUTTNER AND E. N. MASLEN

Department of Physics, University of Western Australia, Nedlands 6009, *Australia*

(*Received* 12 *February* 1988; *accepted* 27 *May* 1988)

Abstract. $KZnF_3$, $M_r = 161{\cdot}47$, cubic, $Pm3m$, $a = 4{\cdot}056$ (1) Å, $V = 66{\cdot}72$ (3) Å^3, $Z = 1$, $D_x = 4{\cdot}018$ Mg m^{-3}, λ(Mo $K\alpha$) = 0·71069 Å, $\mu = 10{\cdot}81$ mm^{-1}, $F(000) = 76$, $T = 298$ K, final $R = 0{\cdot}009$, $wR = 0{\cdot}008$ for 101 unique reflections. The difference density near the Zn atom is not isotropic. The largest peak of 0·38 e Å^{-3} is 0·61 Å from the Zn atom on the Zn–F bond axis. The greatest depletion of –0·56 e Å^{-3} is at the mid point between K atoms. The signs of atomic charges based on the independent atom model (IAM) are consistent with atomic electronegativities but their magnitudes are less than the formal values. The difference density based on the ionic model closely resembles that based on the IAM. The effective charges based on the ionic model are also markedly less than the formal values.

Introduction. Compounds with the formula KMF_3, where M is a divalent metal, have been studied because of their magnetic structure (Hirakawa, Hirakawa & Hashimoto, 1960; Scatturin, Corliss, Elliott & Hastings, 1961). The series provides examples of displacive structural phase transitions (Rousseau, 1979). Recently, interest in $KZnF_3$ has focused on heat-capacity analysis (Burriel, Bartolomé, González, Navarro & Ridou, 1987), in view of its structural stability down to 4 K.

Difference density maps have been obtained for the isomorphic Mn, Fe, Co and Ni structures as well as the Jahn–Teller distorted Cu compound, in connection with studies of spin states of 3*d* electrons (Tanaka, Konishi & Marumo, 1979; Kijima, Tanaka & Marumo, 1981, 1983; Miyata, Tanaka & Marumo, 1983). The focal point of those studies was the redistribution of 3*d* electrons associated with transition metals with incomplete 3*d* subshells. However, there were other significant features in the maps, notably near the F nucleus, but also at the point midway between the K nuclei, which are outside the normal bond radii for all the atoms in the structures. The nature of these features changed markedly through the series Mn, Fe, Co and Ni, the changes also being related to cell size (Spadaccini, 1988). There was strong correlation between the features associated with the transition-metal 3*d* electrons and those elsewhere in the structure. The main problem in explaining those features that correlated was to differentiate cause from effect. That is, did the repopulation of the 3*d* subshell induce polarization at other locations in the structure, or was the correlation because all were produced by the same crystal field?

In order to help resolve this question we have studied the $KZnF_3$ structure. The electron difference density in the Zn compound provides a reference standard for comparison with the transition-metal perovskites studied previously. Because the Zn atom has a filled 3*d* subshell, it is intrinsically less polarizable than that of transition metals with incomplete 3*d* subshells.

Experimental. Crystals of $KZnF_3$ were grown by slow diffusion of 0·6 M KF into 0·2 M $Zn(NO_3)_2$ through a fine capillary over a period of weeks (chemicals suggested by Palmer, 1962). They were washed several times with water and dried. The crystals were found to exhibit a mixture of mainly {100} and {111} faces, the largest being 0·25 × 0·25 × 0·25 mm in size.

The crystal selected for data collection was a deformed octahedron with seven {111} faces and a (211) face (the latter being the area of attachment to

0108-2701/88/101707-03$03.00

Table 1. *Anisotropic thermal parameters, U* ($Å^2 \times 10^5$)

$T = \exp[-2\pi^2 a^{*2}(h^2U_{11} + k^2U_{22} + l^2U_{33})]$, $U_{12} = U_{13} = U_{23} = 0$ as required by symmetry, atomic coordinates Zn 000, K $\frac{1}{2}\frac{1}{2}\frac{1}{2}$, F $\frac{1}{2}00$.

	U_{11}	U_{22}	U_{33}
Zn	691 (5)	691 (5)	691 (5)
K	1507 (7)	1507 (7)	1507 (7)
F	760 (23)	1976 (23)	1976 (23)

glass during growth). The distance of the faces from the centre varied from 0·026 to 0·058 mm. Data were collected on a Syntex $P2_1$ diffractometer. Monochromated Mo $K\alpha$ radiation. Unit-cell dimensions from 6 reflections, $41·02 \le 2\theta \le 41·04°$. Scan type $\omega/2\theta$. Scan speed 4·88° min^{-1}. Scan width 1·7° + 0·7°tanθ. Background measurement 1/3 of scan time. $[(\sin\theta)/\lambda]_{max} = 1·08$ $Å^{-1}$. $-8 \le h \le 8$, $-8 \le k \le 8$, $-8 \le l \le 8$. Six standards measured every 100 reflections, max. variation = 1·7%. Analytical absorption correction applied, transmission factors, max. = 0·53, min. = 0·36. Before absorption correction $R_{int} = 8·5\%$, after $R_{int} = 2·4\%$. $\sum\sigma(I)/\sum(I) = 2·2\%$. 2913 reflections merged to 101 unique reflections. Lorentz and polarization corrections applied. Full-matrix least-squares refinement based on F. Weighting scheme $w = 1/\sigma^2(F_o)$. Anisotropic thermal parameters and isotropic extinction parameter refined (Larson, 1970). Before extinction corrections applied $R = 2·8$, $wR = 2·6\%$, after $R = 0·9\%$, $wR = 0·8\%$, $S = 2·3$ (2). Largest extinction correction = 0·83, with 11 values < 0·99 and 27 < 1·00. $(\Delta/\sigma)_{max}$ in final refinement cycle < 0·0001. Atomic scattering factors of Cromer & Mann (1968) and the anomalous-dispersion corrections of Cromer & Liberman (1970) were used. All calculations were carried out using the *XTAL* system of crystallographic programs (Hall & Stewart, 1987).*

Discussion. Table 1 reports the invariant atomic coordinates and refined anisotropic thermal parameters.

Difference density maps were determined for the (100) plane (Figs. 1*a* and 1*b*) and for the (110) (Fig. 2). The maximum and minimum difference densities are as given in the *Abstract*. Other peaks are 0·23 e $Å^{-3}$ at 0·71 Å from the F atom in a ridge formation of approximately 0·1 Å in length (Fig. 1*a*) and 0·33 e $Å^{-3}$ at 0·61 Å from the K atom (Fig. 2). There is also a deficiency of −0·26 e $Å^{-3}$ centred on the Zn atom as shown in Figs. 1(*a*) and 2. If the result is taken in isolation, the minimum difference density of −0·56 e $Å^{-3}$ at the mid point between K atoms (X,

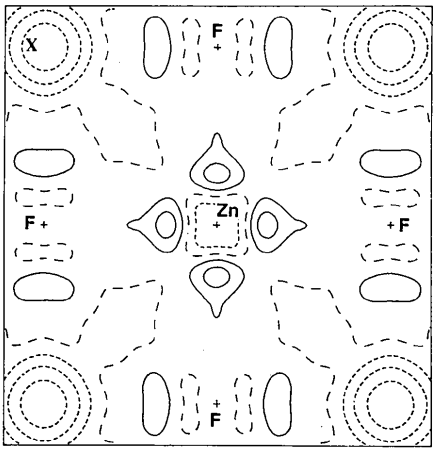

(*a*)

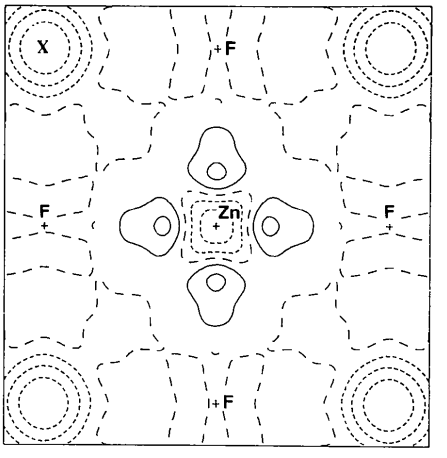

(*b*)

Fig. 1. Fourier difference map for (100) plane in $KZnF_3$ using (*a*) atomic scattering factors, (*b*) ionic scattering factors. Map borders 5·0 by 5·0 Å; contour intervals 0·15 e$Å^{-3}$, positive, zero, negative contours – solid, long and short dashes, respectively.

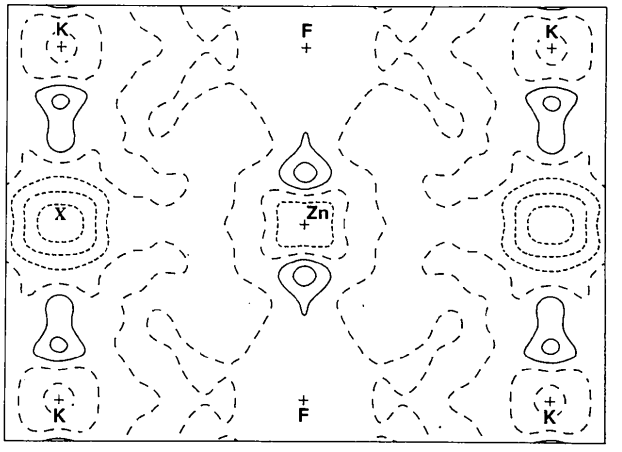

Fig. 2. Fourier difference map for (110) plane in $KZnF_3$. Map borders 7·0 by 5·0 Å; contouring as in Fig. 1.

* Lists of structure factors have been deposited with the British Library Document Supply Centre as Supplementary Publication No. SUP 51103 (2 pp.). Copies may be obtained through The Executive Secretary, International Union of Crystallography. 5 Abbey Square, Chester CH1 2HU, England.

Table 2. *Atomic charges based on Hirshfeld partitioning and IAM*

	Charge (e)
Zn	0·18 (2)
K	0·47 (2)
F	−0·21 (2)

Figs. 1*a* and 2) could be questioned as being an artifact of this analysis. However, the possibility is excluded because similar features appear in the maps of the isomorphic Mn, Fe, Co and Ni compounds. In this structure the e.s.d. in $\Delta\rho$ calculated by the method of Cruickshank (1949) is 0·03 e Å^{-3}. While the K and F atoms are at a distance of $a/2$ from this deficiency, its shape is largely governed by the Zn atoms at a distance of $2^{1/2}a/2$, as shown by troughs formed in Figs. 1(*a*) and 2.

The net charges on each atom, given in Table 2, were determined by the Hirshfeld (1977) partitioning of $\Delta\rho$. They exhibit a significant difference from the usually accepted quantities determined from oxidation states, as observed by other workers (*e.g.* Hirshfeld & Hope, 1980; Baert, Coppens, Stevens & Devos, 1982). However, the signs and relative magnitudes of the charges are consistent with the electronegativities of the atoms in the structure.

A refinement was also carried out using the ionic scattering factors K^+, Zn^{2+} and F^- of Cromer & Mann (1968). The effect was to

(i) Decrease the peak associated with the Zn atom to 0·34 e Å^{-3} with a broadening of this positive difference density region and increase the deficiency at the Zn centre to −0·39 e Å^{-3} (Fig. 1*b*).

(ii) Decrease the F-atom peak to 0·14 e Å^{-3} with an increase in ridge length (Fig. 1*b*).

(iii) Decrease the K-atom peak to 0·30 e Å^{-3} with a slight narrowing of this region.

(iv) Increase the deficiency at the mid point between K atoms to −0·60 e Å^{-3} (X, Fig. 1*b*).

However, these changes are small compared with the size of the significant features. In general, a change from the IAM to the ionic model has little effect on the appearance of the maps.

The net charges on each atom using the Hirshfeld method and the ionic model were Zn = −0·22 (2), K = 0·36 (2) and F = −0·05 (2) e. The fact that these are lower than the formal values of the ions from which the model is constructed is due to overlap and hence cancellation between positive and negative charges. The result highlights the importance of premises made in choosing a reference model. The charges for the model itself, calculated by applying the Hirshfeld method to the difference between the ionic and atomic models, are Zn = 0·40, K = 0·11, F = −0·16 e.

The polarization near the Zn nucleus is significantly aspherical, in spite of the $3d^{10}$ configuration of the Zn atom. This is consistent with the results reported recently for a tetrahedral Zn complex by Ohba, Shiokawa & Saito (1987). However, the polarization is less marked, and differs qualitatively from that near the transition-metal nuclei for the KMF_3 series, for which the polarization is predominantly due to repopulation of the e_g and t_{2g} levels for the 3*d* states. This is expected because that repopulation does not occur in the filled $3d^{10}$ subshell.

On the other hand, the polarization at the structural cavity labelled X in Figs. 1(*a*), 1(*b*) and 2 is consistent with that at the same location in the transition-metal structures. The result shows that this polarization is not induced by the polarization of the divalent metal's subshell. It must originate from the more global aspects of the crystal field in the KMF_3 structure.

One of us (RHB) thanks the Crystallography Centre of the University of Western Australia for the use of their facilities. We thank Associate Professor A. White for his invaluable advice and assistance during the data measurement.

References

Baert, F., Coppens, P., Stevens, E. D. & Devos, L. (1982). *Acta Cryst.* A**38**, 143–151.

Burriel, R., Bartolomé, J., González, D., Navarro, R. & Ridou, C. (1987). *J. Phys. C*, **20**, 2819–2827.

Cromer, D. T. & Liberman, D. (1970). *J. Chem. Phys.* **53**, 1891–1898.

Cromer, D. T. & Mann, J. B. (1968). *Acta Cryst.* A**24**, 321–324.

Cruickshank, D. W. J. (1949). *Acta Cryst.* **2**, 65–82.

Hall, S. R. & Stewart, J. M. (1987). Editors. *XTAL*2.2 *User's Manual*. Univ. of Western Australia, Australia, and Univ. of Maryland, USA.

Hirakawa, K., Hirakawa, K. & Hashimoto, T. (1960). *J. Phys. Soc. Jpn*, **16**, 2063–2068.

Hirshfeld, F. L. (1977). *Isr. J. Chem.* **16**, 198–201.

Hirshfeld, F. L. & Hope, H. (1980). *Acta Cryst.* B**36**, 406–415.

Kijima, N., Tanaka, K. & Marumo, F. (1981). *Acta Cryst.* B**37**, 545–548.

Kijima, N., Tanaka, K. & Marumo, F. (1983). *Acta Cryst.* B**39**, 557–561.

Larson, A. C. (1970). *Crystallographic Computing*. Copenhagen: Munksgaard.

Miyata, N., Tanaka, K. & Marumo, F. (1983). *Acta Cryst.* B**39**, 561–564.

Ohba, S., Shiokawa, K. & Saito, Y. (1987). *Acta Cryst.* C**43**, 189–191.

Palmer, W. G. (1962). *Experimental Inorganic Chemistry*, pp. 178–181. Cambridge Univ. Press.

Rousseau, M. (1979). *J. Phys. Lett.* **40**, L439–443.

Scatturin, V., Corliss, L., Elliott, N. & Hastings, J. (1961). *Acta Cryst.* **14**, 19–26.

Spadaccini, N. (1988). PhD Thesis, Univ. of Western Australia, Australia.

Tanaka, K., Konishi, M. & Marumo, F. (1979). *Acta Cryst.* B**35**, 1303–1308.